

Loudspeaker voice-coil temperature estimation

Ronny Andersson

Luleå University of Technology
MSc Programmes in Engineering
Electrical Engineering
Department of Computer Science and Electrical Engineering
Division of Signal Processing

Loudspeaker voice-coil temperature estimation

MASTER'S THESIS - ELECTRICAL ENGINEERING

Ronny Andersson
ronand-0@student.ltu.se

March 8, 2008



Abstract

The temperature in the voice-coil of a loudspeaker is an important variable in the sense of protection against failure. In order to estimate the temperature in the voice-coil an adaptive filter has been used. The adaptive filter utilises a *system identification* setup. The impulse response of the loudspeaker is estimated and the impedance of the loudspeaker can therefore be derived. This is performed while the loudspeaker is under normal use, that is, with music as input. A curve fitting is performed on the impedance derived from the adaptive filter. This is done in order to describe the loudspeaker with its linear parameters. The relationship between the DC-resistance of the loudspeaker voice-coil and temperature is well-known. Therefore the temperature can be derived when the impedance is known. The accuracy of the system described in this thesis is not good enough for correctly estimating the temperature but this is believed to be measurement errors.

Contents		
1 Introduction	3	6 Future work 19
1.1 Purpose	3	
1.2 The loudspeaker	3	7 Acknowledgements 19
1.3 Modelling	4	A Adaptive filter theory 21
1.3.1 Electromechanical modelling	4	A.1 Least Mean Square 21
1.3.2 Thermal modelling	5	A.2 Normalised Least Mean Square 22
1.4 Thermal compression	6	B Function minimisation 22
1.5 Resonance frequency	6	B.1 Nelder–Mead algorithm 22
2 Adaptive parameter estimation	7	
3 Measurements	7	
3.1 Recording and sampling	7	
3.2 Electronics	7	
3.2.1 Voltage measurement	8	
3.2.2 Current measurement	8	
3.2.3 Calibration	9	
3.3 Temperature measurement	10	
3.3.1 Thermocouple theory	10	
3.3.2 Verification of type	10	
3.3.3 Step response	11	
4 Processing of measurements	11	
4.1 Scaling	11	
4.2 Downsampling	11	
4.3 Adaptive filter	12	
4.3.1 Filter parameters	13	
4.3.2 Error minimisation	14	
4.3.3 Impulse response processing	14	
4.4 Curve fitting	15	
4.5 Temperature calculations	16	
4.6 Resonance frequency shift	17	
5 Analysis and discussion	18	
5.1 Verification of results	19	

Glossary of symbols

B	Magnetic flux density in driver air gap
l	Length of voice-coil conductor in magnetic field B
i	Instantaneous current
R_e	DC coil resistance
L_e	Coil inductance
C_{mes}	Electrical capacitance due to driver mass, including the air load
L_{ces}	Electrical inductance due to the suspension compliance
R_{es}	Electrical resistance due to driver suspension losses
T	Temperature in °C
$R_e(T)$	DC coil resistance as a function of temperature
T_0	Ambient temperature
$R_e(T_0)$	DC coil resistance R_e at temperature T_0
α	Thermal coefficient, $4.33 \cdot 10^{-3} \text{ K}^{-1}$ for Cu.
Z	Impedance
ω	Frequency in rad/s
j	Imaginary unit, $\sqrt{-1}$
S_d	Surface area of the diaphragm
f_s	Resonance frequency of mechanical system
Q_{es}	Ratio of voice-coil DC resistance to reflected motional reactance at f_s
C_{as}	Acoustic compliance due to the suspension compliance
M_{as}	Acoustic mass of driver diaphragm, including the air load and voice-coil mass
β	Gain
τ	Time constant
$A(s)$	Admittance = 1/impedance
u	Input applied to the adaptive filter
y	Output from the adaptive filter
d	Desired response
e	Estimation error $e = d - y$
μ	Step-size
IIR	Infinite Impulse Response
FIR	Finite Impulse Response
LMS	Least Mean Square
NLMS	Normalised Least Mean Square
$\hat{\mathbf{w}}[n]$	Tap-weight vector (coefficients for FIR filter) at time n

1 Introduction

The moving coil loudspeaker has been around for hundred years now, and still it is based on the same physical principles. Improvements has been made mostly in the materials used. Other types of loudspeakers has been developed, such as the electrostatic loudspeaker, piezoelectric loudspeaker and the ribbon loudspeaker. But still the moving coil loudspeaker is the most commonly used loudspeaker. The fidelity of the moving coil loudspeaker is good for a wide frequency range. The electrostatic and piezoelectric loudspeakers are limited to higher frequencies, due to high mechanical impedance for the piezoelectric loudspeaker and high polarisation voltage for the electrostatic speaker.

The efficiency for the moving coil loudspeaker is surprisingly low, around 5% of the energy that is put into a moving coil loudspeaker is transformed into sound, the rest is transformed into heat.

The focus of this thesis is on the moving coil direct-radiator loudspeaker, hereafter only referred to as the *loudspeaker*.

1.1 Purpose

Due to the low efficiency of the loudspeaker, where 95% of the energy delivered to the loudspeaker is turned into heat it is important to be aware of the temperature inside the loudspeaker. The main source of the heat is the voice-coil. The other source is eddy currents in the magnet structure.

In other words, to achieve high sound pressure levels the loudspeaker needs to be inputted with high power, which therefore results in an increase of the temperature. A high input also results in a large displacement of the loudspeaker membrane, which then can result in a mechanical damage.

Therefore it is important to consider the temperature of the voice-coil for the purpose of protection.

Other effects of the temperature change in the voice-coil is thermal compression, which will be explained briefly in section 1.4.

1.2 The loudspeaker

The *moving coil loudspeaker* consists of a moving coil inside a static magnetic field, where the coil is connected to a membrane. A current in the coil produces a magnetic field around the wire which will move the coil. This is described by King [1].

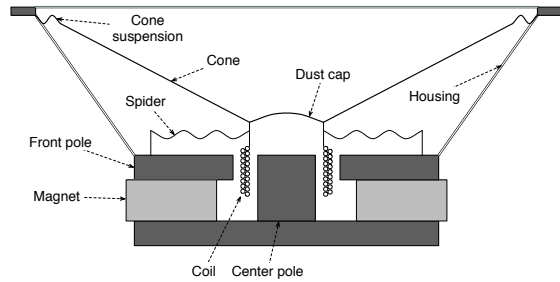


Figure 1: *General purpose loudspeaker. Not to scale.*

Figure 1 shows a general purpose loudspeaker. With the aid of figure 2 the force applied on the coil can be predicted. The flux path is shown in figure 3. The force on the coil produces a motion that is transformed to the cone and thereafter the air.

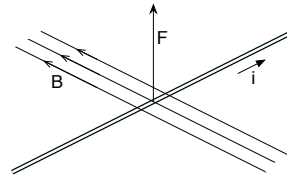


Figure 2: *Force due to magnetic flux and DC-current.*

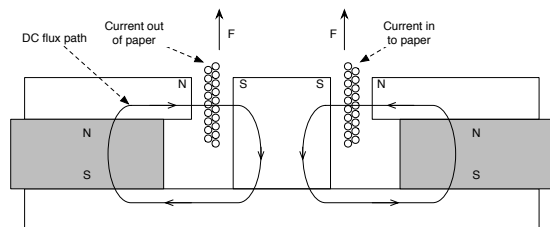


Figure 3: *DC flux flow shows resulting force.*

The instantaneous force F has the value

$$F = Bl \cdot i \quad (1)$$

where B is the magnetic flux density and l is the length of the voice-coil in the magnetic field and i is the instantaneous current. The current i can be held fixed but the magnetic flux B and the length l in the magnetic field will vary whenever some portion of the coil is outside the magnetic field B . This is one of the many nonlinearities in loudspeaker modelling.

The axial length of the coil is a design choice, but the advantages of using a coil that has a length *greater* than the axial magnetic gap is discussed by King [1] and this is still today the preferred choice.

1.3 Modelling

The loudspeaker behaviour can be modelled differently depending on what kind of information is desired. The two popular models are the *electromechanical* model and the *thermal* model.

The thermal behaviour can somewhat be extracted from the electromechanical model and the temperatures from the thermal model can provide useful information into the electromechanical model. In other words, the two models complement each other.

1.3.1 Electromechanical modelling

The electromechanical model is described by Thiele [2, 3] and Small [4, 5, 6] which has resulted in the today well-known *Thiele-Small parameters*. Some important restrictions must be mentioned first:

- The model is *linear*.
- It is valid in the *piston range* which means that the wavelength of sound is longer than the circumference of the driver diaphragm.
- To be practical to use it is simplified to a *lumped* parameters model, which means that several parameters are lumped together to behave as one.

The importance of the first item cannot be stressed enough, since the loudspeaker has a nonlinear behaviour even at a small displacement of the diaphragm.

The complete electromechanical model described in [2] and in [4] is simplified to the electrical equivalent circuit in figure 4.

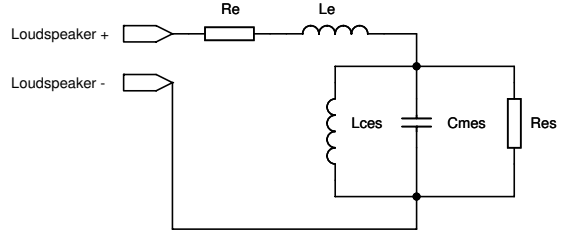


Figure 4: *Simplified electrical equivalent loudspeaker model.*

The lumped parameters in figure 4 describes the electrical behaviour in the simplest manner.

The parameter R_e is the DC coil resistance, which according Behler [7] is the only temperature-dependant part and therefore more correctly should be expressed as $R_e(T)$, that is, as a function of temperature. This parameter is directly related to the temperature according to

$$R_e(T) = R_e(T_0)(1 + \alpha(T - T_0)) \quad (2)$$

where $\alpha = 4.33 \cdot 10^{-3} \text{ K}^{-1}$ for copper. The linear relationship of R_e as a function of temperature can be seen in figure 5.

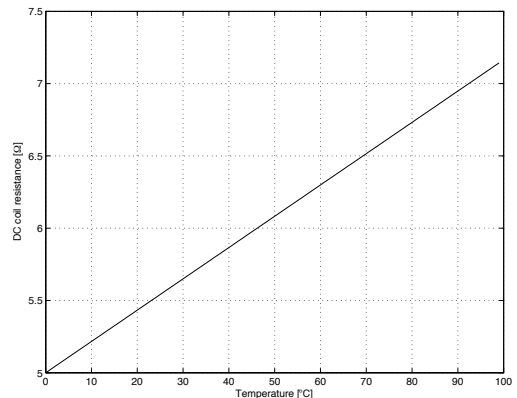


Figure 5: *Model parameter R_e as a function of increasing temperature*

An increase in temperature by 50°C results in an increase in R_e by approximately 1Ω .

The parameter L_e is the coil inductance. This is a very simple lumped parameter, and various attempts has been made to correctly model the behaviour at high frequencies. Vanderkooy

[8] suggests that the impedance has a behaviour given by

$$Z = K\sqrt{j\omega} \quad (3)$$

where the constant K is the semi-inductance in semihenrys.

Wright [9] suggests an empirically derived model, where the impedance is given by the expression

$$Z = K_r\omega^{X_r} + jK_i\omega^{X_i} \quad (4)$$

where the subscripts r and i stand for Real and Imaginary parts. The method of finding the constants K_r , X_r , K_i and X_i is based on two different measurements of the impedance at two high frequencies. This results in a frequency-dependant resistor and a frequency-dependant inductor in series,

$$R_{em} = K_r\omega^{X_r} \quad (5)$$

and

$$L_{em} = K_i\omega^{X_i-1}. \quad (6)$$

Leach [10] proposes another model, where a frequency-dependant inductor and a frequency-dependant resistor in parallel with values

$$R_p = \frac{K\omega^n}{\cos(n\pi/2)} \quad (7)$$

and

$$L_p = \frac{K\omega^{n-1}}{\sin(n\pi/2)} \quad (8)$$

gives the desired behaviour. The values of the constants K and n are found using curve fitting methods on a measured impedance.

Wu [11] compares three different models with measurements and claims that the model by Wright is the most accurate one.

The simple lossless inductor L_e in series with R_e seems to be all too inadequate to model the high-frequency behaviour but for this thesis it is used. The frequency response at high frequencies is of little importance in the method described later, and therefore the simple inductor is used.

C_{mes} is the electrical equivalent capacitance due to the mass of the driver diaphragm assembly, including the air load and the mass of the voice-coil.

L_{ces} is the electrical equivalent inductance due to the suspension compliance. Compliance is equal to the reciprocal of stiffness.

R_{es} is the electrical equivalent resistance due to driver suspension losses.

The three parameters C_{mes} , L_{ces} and R_{es} are all derived from the complete electromechanical model. The conversion from mechanical/acoustical to electrical equivalent is performed using S_d^2 (the squared surface area of the diaphragm) and $(Bl)^2$. This is described in Small [4]. This means that the three parameters are linear whenever Bl is constant, but as described in section 1.2 it can vary, and therefore all parameters must be regarded as linear only at a small displacement. This also means that at large displacements all parameters will be nonlinear and change as a function of displacement.

The theoretical impedance from the model in figure 4 can be described in the s-plane as

$$Z(s) = R_e + sL_e + \left(\frac{1}{sL_{ces}} + sC_{mes} + \frac{1}{R_{es}} \right)^{-1} \quad (9)$$

Eq 9 has the form

$$Z(s) = \frac{s^3a_1 + s^2a_2 + sa_3 + a_4}{s^2b_1 + sb_2 + b_3} \quad (10)$$

where a_i and b_i are different constants. This is important to realise, because solving equation 10 yields that there is more zeros than poles.

Using equation 9 with the substitution $s = j\omega$ and using some typical values for the different parameters yields the theoretical impedance shown in figure 6. This is a typical (theoretical) response for a woofer type loudspeaker.

The parameter R_e is frequency-independent and is therefore responsible for the general offset. The parameters C_{mes} , L_{ces} and R_{es} are responsible for the resonance peak at frequency f_s . At that frequency the values of C_{mes} and L_{ces} cancel each other and the magnitude of the peak is determined by $R_e + R_{es}$. The rise in impedance at high frequencies is due to L_e .

A method for finding the parameters from an impedance plot is described in [4].

1.3.2 Thermal modelling

The other popular way of estimating the temperature in the loudspeaker is by using a ther-

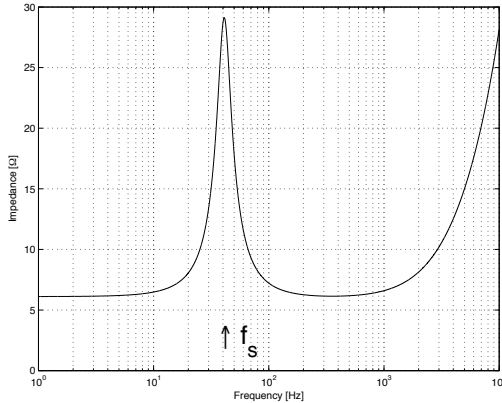


Figure 6: *Theoretical typical impedance of woofer loudspeaker.*

mal model. This is based on the thermal behaviour of the loudspeaker, seen as a lumped component. The main ideas are presented here, only as an orientation on the subject, since the rest of this thesis is based on the electromechanical model described in section 1.3.1.

One model is developed by Henricksen [12]. The model is based on the heat transfer mechanism generally in the form

$$T_d = QR \quad (11)$$

where T_d is the temperature drop across the element, Q is the heat power passing through the element and R is the thermal resistance of the element.

The heat stored in a thermal element is expressed as

$$dE = cmdT \quad (12)$$

where E is the thermal energy stored, c is the specific heat of element, m is the mass of the element and dT is the temperature change of element.

Henricksens model is improved by Chapman [13]. This model is then used in a complete thermal protection system described in a paper by Chapman [14].

The model described by Chapman is slightly different from the model by Henricksen. The improvement is in the way the temperature of the magnet is calculated. Chapman accounts for the presence of the voice-coil, which Henricksen does not.

Another model is described by Blasizzo [15]

where the power dissipated by eddy currents in the pole piece is taken into account.

Klippel [16] has done some extensive work in nonlinear modelling. The model is depending on the displacement x of the diaphragm in order to nonlinearly model the heat flow.

The purpose of the above described models are to accurately estimate the temperature at different places inside the loudspeaker. In order to do so, an estimate of the power delivered into the loudspeaker needs to be calculated.

1.4 Thermal compression

Button [17] investigates the sources of thermal compression. When R_e increases, Button describes that three effects take place:

- The electrical Q_{es} rises, decreasing electromechanical damping.
- The half-space efficiency decreases, reducing expected output.
- The impedance rises and voltage sensitivity will decrease.

The combination of the above items is called *thermal compression*. These are of course unwanted side effects. The Thiele-Small parameter Q_{es} is defined as the ratio of voice-coil DC resistance to reflected motional reactance at f_s , or expressed with the electromechanical parameters,

$$Q_{es} = 2\pi f_s C_{mes} R_e. \quad (13)$$

As R_e increases Q_{es} will increase. The other two items in the list of the sources of thermal compression can be explained simply by that an increasing R_e at a constant voltage will result in a lower current through the loudspeaker, resulting in a lower acoustic output.

1.5 Resonance frequency

The resonance frequency f_s will shift to a lower frequency when a large input signal is applied to the loudspeaker. This will be shown from measurements in section 4.6.

The resonance frequency f_s is defined as

$$f_s = \frac{1}{2\pi} \sqrt{\frac{1}{C_{as}M_{as}}} \quad (14)$$

where C_{as} is the acoustic compliance and M_{as} is the acoustic mass (electric equivalent is L_{ces} and C_{mes}). When the loudspeaker is excited with a large input signal the displacement is large. One possible explanation to the shift of resonance frequency is that large displacement of the diaphragm increases the compliance. Remember that compliance is the reciprocal of stiffness. If C_{as} is increased then by equation 14 the resonance frequency f_s will decrease.

2 Adaptive parameter estimation

A different approach of estimating the temperature is hereby presented. Since the parameters of the loudspeaker model described in section 1.3.1 changes when the loudspeaker is used there is a need for a real-time update of the estimation of the parameters. The parameter that changes most dramatically is R_e due to the increase of temperature in the voice-coil. But the compliance L_{ces} also changes when the whole loudspeaker heats up. The rubber surroundings softens due to mechanical fatigue and therefore the compliance increases, contributing to the resonance frequency shift described in section 1.5.

The magnetic flux B also changes with increasing temperature. Button [17] reports a 10% loss in magnetic flux for a neodymium magnet at a temperature change of $\approx 100^\circ\text{C}$.

Remember that the conversion from acoustical to electrical parameters includes $(Bl)^2$. This means that all the linear parameters, C_{mes} , L_{ces} and R_{es} , changes with increasing temperature.

The idea behind *adaptive parameter estimation* is to continuously measure voltage and current and calculate the impedance. The calculation of the impedance is done by using an adaptive filter to identify the loudspeaker impulse response. The impulse response is then used to calculate the frequency response, and thereafter a curve fit is performed on the estimated impedance. The curve fit is performed by modifying the model parameters until they fit the

measured impedance. This results in an estimation of all the linear parameters.

This is a relatively new way of estimating the loudspeaker model parameters. A paper presented by Pedersen [18] basically describes the same approach of finding the parameter values. The results found in this report overlaps the results by Pedersen.

3 Measurements

In order to estimate the parameters some variables need to be measured. The only practical variables to measure are the instantaneous current i and the instantaneous voltage v over the loudspeaker. To verify the estimated temperature the actual temperature inside the voice-coil is measured. The hardware setup for the measurements is shown in figure 7.

The generated signal is fed through a class-AB power amplifier and into a loudspeaker mounted on a baffle. The voltage and current is measured and recorded into a computer. The actual temperature is recorded into the same computer.

3.1 Recording and sampling

A standard MOTU¹ 896HD soundcard is used to record the voltage and the current. In order to do so, some electronics was built to scale the levels. The sampling frequency used is 44.1 kHz and the bit-depth is 24 bit. The recordings are done directly into Matlab² using the open source extension `pa_wavplay`³.

3.2 Electronics

The gain β_0 of the power amplifier in figure 7 is different from different manufacturers, but it can be 20-40 dB for a professional power amplifier. Using

$$G_{dB} = 20 \log_{10} \left(\frac{v_1}{v_0} \right) \quad (15)$$

which can be rewritten as

$$v_1 = v_0 \cdot 10^{\frac{G_{dB}}{20}} \quad (16)$$

¹<http://www.motu.com>

²<http://www.mathworks.com>

³<http://sourceforge.net/projects/pa-wavplay/>

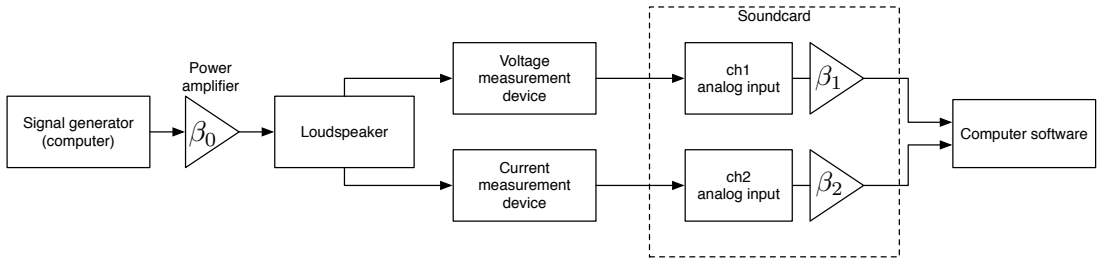


Figure 7: *Hardware setup for measurements.*

it can be seen that an input voltage v_0 of $1 V_{rms}$ and a gain of 26 dB will generate an output voltage of approximately 20V. If the loudspeaker is rated at 4Ω , the approximate current will be 5A. In order to use a standard soundcard as a recording device the signal needs to be attenuated. The input of a soundcard typically handles a maximum of a couple of volts.

3.2.1 Voltage measurement

The simple circuit shown in figure 8 was built to be able to record the voltage directly into a soundcard.

The circuit consists of a voltage divider with the two resistors R_1 and R_2 . The voltage between the two resistors is calculated as

$$v_{div} = v_{sp} \frac{5,9k}{590k + 5,9k} = v_{sp} \frac{1}{101} \quad (17)$$

where v_{sp} is the voltage over the speaker and v_{div} is the voltage between the two resistors and k is kilo= 10^3 . The two resistors have a tolerance of 1%.

This results in a voltage output that is a factor 101 lower than the voltage over the loudspeaker. The voltage is fed into an OP-amplifier (OPerational amplifier) connected as a voltage follower, with a gain of one. This is used for separating the loudspeaker from the soundcard.

3.2.2 Current measurement

The circuit in figure 9 was built to measure current. Resistor R_7 is connected as a shunt in series with the loudspeaker, so that the current can be measured.

The value of R_7 is known, and when current

flows through it the voltage drop can be measured and the current can be calculated.

The OP-amplifier is connected as a differential amplifier and has a gain of one.

Some restrictions on R_7 are worth mentioning;

- The value has to be low enough not to raise the total impedance too much.
- The resistor has to be able to withstand the high current through the loudspeaker.

The first item is no problem, since the known resistance can be subtracted from the calculated impedance.

The second item is more important. A high current will eventually lead to a relatively high power dissipation in the resistor. If the resistor gets warm it will change its resistance according to equation 2 with the proper value of α .

To minimise the effect of heating, R_7 is actually an array of ten equal power-resistors connected in parallel to result in an $R_{equivalent} = R_7 = 0.190\Omega$. The array is mounted so that each resistor have approximately 1 cm to its neighbour. A standard air-fan was put in front of the array to ensure proper airflow.

The current is therefore calculated as

$$i_{sp} = \frac{v_{out}}{0.190} \quad (18)$$

where v_{out} is the voltage output from the OP-amplifier and i_{sp} is the current through the loudspeaker.

This is the second design for the current measurement circuit. The first design suffered from an $R_{equivalent}$ that just barely handled the power developed and therefore increased in temperature. This resulted in measurements where

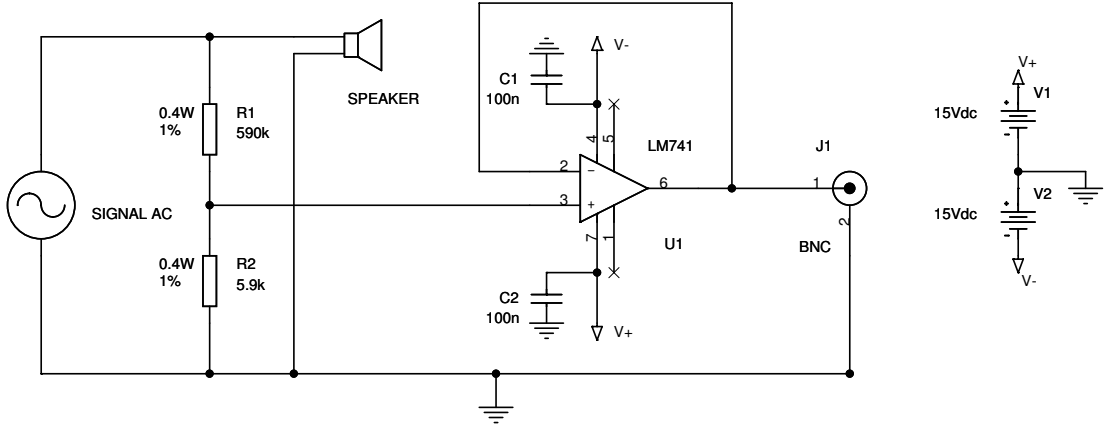


Figure 8: *Electronics for measuring the voltage over the loudspeaker.*

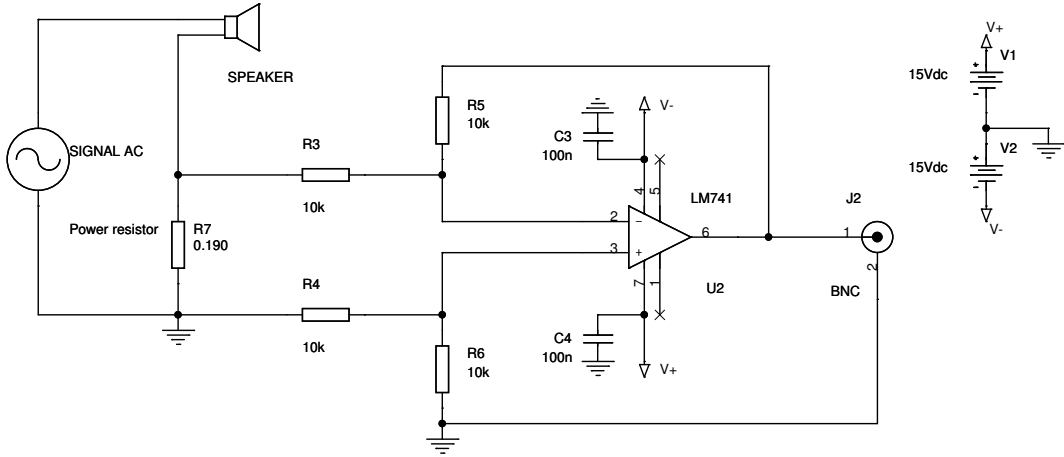


Figure 9: *Electronics for measuring the current through the loudspeaker.*

both the model parameter R_e and shunt resistor R_7 changed with increasing temperature. This made one week of measurements useless.

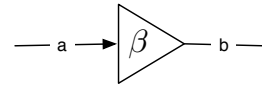


Figure 10: *Determination of unknown gain β .*

3.2.3 Calibration

A gain calibration procedure was performed to find the unknown gains β_1 and β_2 in figure 7. This is necessary in order to work with the correct units of voltage and ampere in the processing described later. The problem can be simplified down to figure 10.

A calibration signal consisting of a sinusoid at 1kHz is fed to the input of the soundcard. The voltage a in RMS is measured with a digital multimeter. The recorded signal b has an RMS

value that is calculated on N samples x as

$$b_{rms} = \sqrt{\frac{1}{N} \sum_{i=1}^N x_i^2}. \quad (19)$$

The gain β is then found by calculating

$$\beta = \frac{b_{rms}}{a_{rms}}. \quad (20)$$

3.3 Temperature measurement

The actual temperature inside the voice-coil was measured using a custom made Peerless woofer loudspeaker fabricated by Tymphany⁴. The woofer has a type J thermocouple wounded into the voice-coil and another type J thermocouple mounted directly onto the magnet to monitor the temperatures. Both thermocouples were connected to an Agilent⁵ 34970A Data Acquisition Switch Unit. This allowed the temperature to be monitored at specified intervals. For this thesis a sampling period of one second was used.

3.3.1 Thermocouple theory

A thermocouple sensing element (as described in Bentley [19]) consists of two different metals A and B joint together in a junction. Between the two metals there is a voltage difference that is called the *junction potential*. The junction potential is depending on the temperature T [°C] at the junction and has a nonlinear behaviour approximated by the polynomial

$$E_T^{AB} = \sum_{n=1}^N a_n T^n \quad (21)$$

where the coefficients a_n is different depending on the two metals A and B . The choice for N depends on how accurate the nonlinearity should be approximated.

Different types of thermocouples exist, the ones used in this thesis is the type K and type J. The type K consists of the two alloys Chromel and Alumel and has a range of 0 to +1000 °C. The type J consists of Iron and the alloy Constantan and has a range of -20 to +700 °C. Both thermocouples have a tolerance of $\pm 1.5^\circ\text{C}$.

The two thermocouples have voltage values E shown in figure 11.

3.3.2 Verification of type

The custom made woofer was manufactured some ten years ago and unfortunately the documentation has been lost. Since there were two thermocouples of the same type used and the

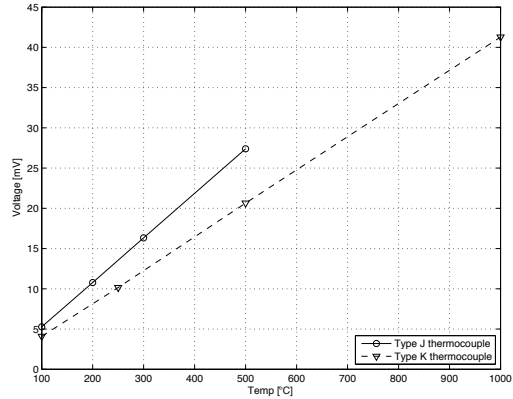


Figure 11: *Thermocouple sensitivity.*

one on the magnet was easily accessible it was removed for a verification of device type.

In order to verify that the thermocouple is a type J, a calibration device⁶ was used to produce two different fixed temperatures. The device was set to a temperature of 60°C and after a while it was manually changed to 70°C. The calibration device has an error less than 1°C. The temperature in the calibration device was read both on the display of the device and also measured with a type K thermocouple. The type K thermocouple was a green/white (IEC standard) thermocouple and it was also connected to the data acquisition unit. The two different temperatures are shown in figure 12.

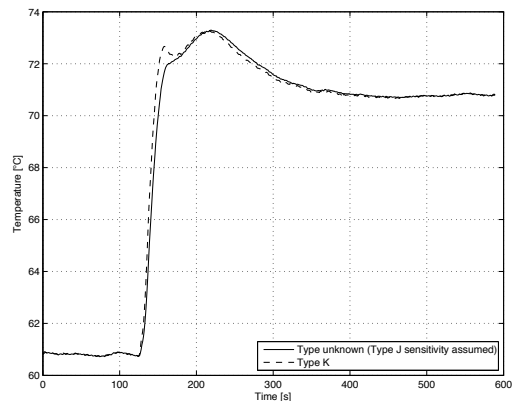


Figure 12: *Verification of thermocouple types, utilising a special device with two different known temperatures.*

The figure shows that both thermocouples fol-

⁴<http://www.tymphany.com>

⁵<http://www.home.agilent.com>

⁶A box that delivers a precise adjustable known temperature in a small metallic hole.

low each other and closely matches the correct temperatures of 60°C and 70°C.

The two thermocouples used in the woofer are therefore *verified as to be of type J*.

3.3.3 Step response

The step response of the type J thermocouple (and also at the same time the type K thermocouple) was investigated by simply increasing the temperature from room-temperature to a higher temperature by placing it between two fingers. Figure 13 shows the rise and performing a simple analysis on the figure reveals that the time constant⁷ for the thermocouple is $\tau \approx 1$ s.

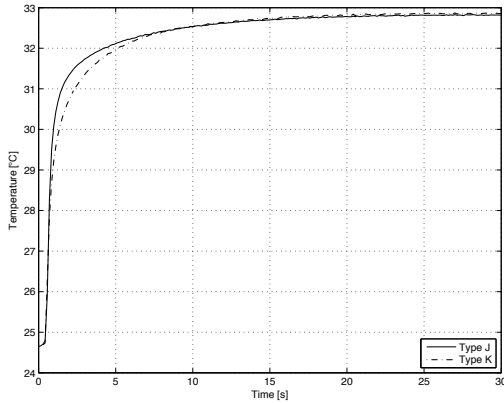


Figure 13: *Step response of type J and type K thermocouples.*

This means that the time constant for the thermocouple used is much shorter than the shortest time constant in the loudspeaker used in this thesis. The thermal time constant for that voice-coil is somewhere around 10s (Chapman [13]). The thermocouple is therefore fast enough not to influence the measurements of the loudspeaker temperature.

4 Processing of measurements

The measurements described in section 3 are all processed and analysed in Matlab. The recordings of the voltage and the current are done di-

⁷The time it takes for a system to reach approximately 63% of its final value when a step is applied.

rectly in Matlab whereas the temperature measurements are exported as a comma-separated file and manually imported and time synchronised with the voltage and current. A sampling period of one second was used for the temperature measurements and therefore the synchronisation can off by a maximum of ± 1 s.

The general flow for the Matlab processing is shown in figure 14.

4.1 Scaling

The gains calculated in section 3.2.3 are used to scale the measurement to the correct values. This means that the correct units of V and A can be used in all calculations. The principles in equation 17 are used and the correct voltage is therefore calculated as

$$v_{correct} = 101 \frac{v_{rec1}}{\beta_1} \quad (22)$$

where v_{rec1} is the recorded signal from channel 1.

Similarly equation 18 is used to calculate the correct current as

$$i_{correct} = \frac{1}{0.190} \frac{v_{rec2}}{\beta_2} \quad (23)$$

where v_{rec2} is the recorded signal from channel 2.

4.2 Downsampling

For the purpose of identifying four of the five parameters describing the loudspeaker there is no need for a full frequency bandwidth using a samplerate of 44.1kHz. The resonance frequency of a woofer relatively low, usually below 300Hz. The inductance L_e is of less importance and therefore it can be disregarded.

Another reason for downsampling is that the frequency resolution at low frequencies is increased.

For this purpose a downsampling factor of 20 is applied. The new sampling-frequency is therefore $44100/20=2205$ Hz. This is good enough to accurately describe four of the loudspeaker parameters. Due to the anti-aliasing filter applied in the downsampling process the highest frequencies cannot be trusted, and therefore the value of L_e will be estimated wrongly.

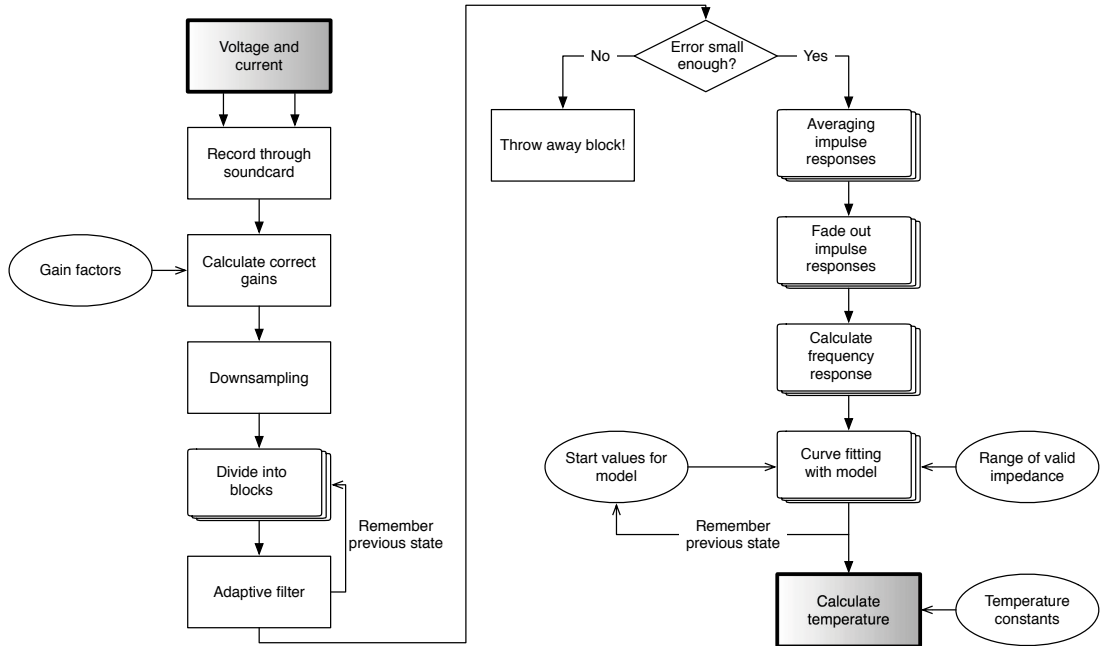


Figure 14: *Flow of processing in Matlab.*

4.3 Adaptive filter

In order to identify the loudspeaker system an adaptive filter is used. The theory about adaptive filters is described in details by Haykin [20] and a brief summary is presented in appendix A.

Figure 15 shows a *system identification* adaptive filter setup. This is used when both the input and the output can be accessible and the system is *unknown*. From this viewpoint the loudspeaker behaviour is unknown but it is assumed to be linear. The linearity assumption will later show up to be a problem.

The loudspeaker impedance described by equation 9 can be more conveniently expressed as the admittance

$$A(s) = \frac{1}{Z(s)}. \quad (24)$$

The current $I(s)$ can therefore be expressed as

$$I(s) = \frac{V(s)}{Z(s)} = V(s)A(s). \quad (25)$$

Filtering the voltage $V(s)$ with a filter that has the same impulse response as $A(s)$ will then result in the current $I(s)$. This is what the adaptive filter does in order to find an estimation of

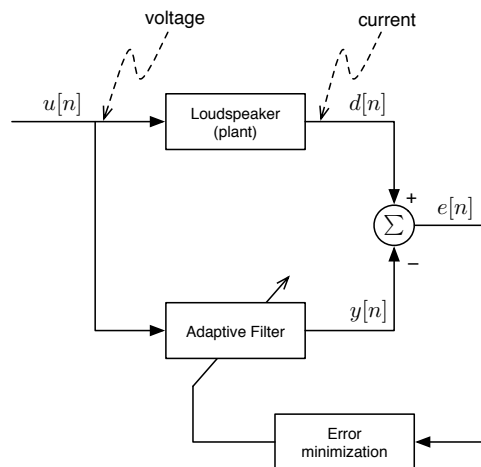


Figure 15: *Adaptive filter for estimating the admittance.*

the impulse response of the loudspeaker. The difference between the actual measured current i , defined as the desired signal, and the adaptive output y (estimated current) is called the error e , defined as

$$e = d - y. \quad (26)$$

When the error e is small enough the impulse response of the adaptive filter describes the be-

behaviour of the loudspeaker. The frequency response of the adaptive filter is actually the admittance but that is just the inverse of the impedance as described in equation 24.

The adaptive filter is implemented in Matlab using `adaptfilt` in the `Filter Design Toolbox` and for implementation issues the input signal is divided into non-overlapping blocks, shown in figure 16. This results in an estimation of the impulse response at the end of each block. This is because of the Matlab implementation and in a sample-by-sample implementation an estimation of the impulse response vector $\hat{\mathbf{w}}$ will be present at each sample.

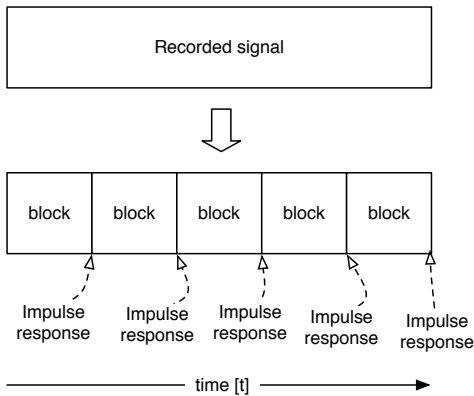


Figure 16: *Recorded signal divided into blocks, for easy implementation. An impulse response is presented at the end of each block.*

The length of one block determines how often an impulse response estimation should be presented. This is a design choice and different intervals have been used in this thesis. In the sense of computational speed there is no change in speed using different block sizes. This is because the vector $\hat{\mathbf{w}}[n]$ will in some sense always be present. The only reason for using a small block size is for further processing, for example averaging which will be discussed in section 4.3.3.

Of course a small block size has the advantage of being able to track fast changes, but this is not the intent in the above discussion.

There exists adaptive filters that are based on an Infinite Impulse Response filter, IIR, but due to the very nature of an adaptive filter that changes its parameters, stability cannot be guaranteed

in an IIR setup. Therefore a Finite Impulse Response, FIR, filter is used. The taps, or coefficients, for an FIR filter is the same as its impulse response.

4.3.1 Filter parameters

Two parameters has to be determined in order to use the adaptive filter. The first is the number of taps, or the length of the impulse response. The second is the step-size μ .

The length of the adaptive filter must be long enough to completely cover the whole impulse response. Applying an impulse on equation 9 results in figure 17. The y-axis has been heavily zoomed in order to really emphasise the fact that the impulse has somewhat died out after 40-50ms.

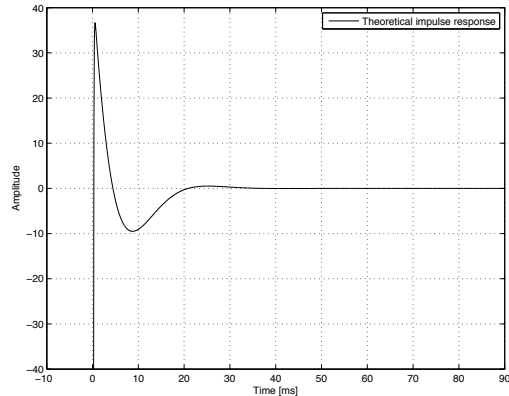


Figure 17: *Impulse response of loudspeaker model (linear). Zoomed y-axis.*

A filter length of 400 was chosen. With a samplerate of 2205 Hz this results in a filter that is $\frac{1}{2205} \cdot 400 \approx 180$ ms long, well enough to capture the whole impulse of the loudspeaker.

To update the taps, or impulse response, the Normalised Least-Mean Square (NLMS) algorithm is used. The NLMS is described in appendix A.2. The step-size μ is determined experimentally. A big step-size means that the filter becomes unstable and a small step-size means that the error converges too slowly to its minimum value. A step-size $\mu = 0.18$ was chosen.

4.3.2 Error minimisation

At the end of each block the impulse response $\hat{\mathbf{w}}$ and the error e is present for further analysis. A plot over a typical error e , adaptive output y and desired signal d is shown in figure 18. The input u is pink noise⁸ and this is a measurement of a real loudspeaker.

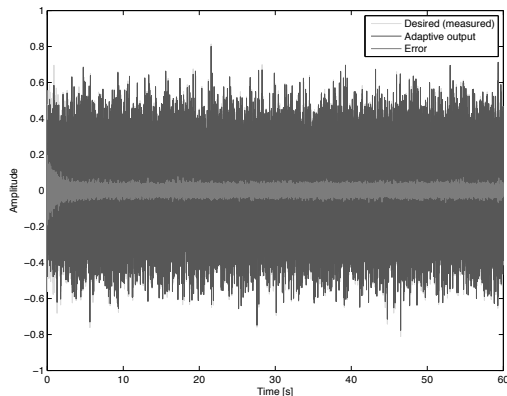


Figure 18: *Error of adaptive filter, real loudspeaker with pink noise as input.*

Figure 18 shows that the magnitude of the error is relatively large compared to the desired signal. A smaller step-size μ would be the first solution to this but unfortunately it is not that easy. The solution is to simply accept that the error does not become smaller. This is explained by the fact that the adaptive filter is a *linear* filter whereas the loudspeaker behaves nonlinear even at a small displacement. To prove this assumption a circuit was built that consisted of the four loudspeaker parameters R_e , C_{mes} , L_{ces} and R_{es} in figure 4. The actual values of these parameters are either small or big compared to "normal", and the power consumption also needs to be taken into account. The inductance L_{ces} was constructed by using one of the windings in a quite big power supply transformer. The inductance and the capacitance would have a DC resistance in series also, so the circuit is not exactly as in figure 4. The point here is that this circuit is *linear*. The linearity of a big iron-core coil could of course be discussed, but it will be more linear than the loudspeaker.

Using the same setup and simply exchanging the

⁸Pink noise is white noise passed through a filter that has a -3 dB per octave roll-off. This is more similar to music than white noise.

loudspeaker with the linear circuit and applying (different) pink noise with the same magnitude results in figure 19.

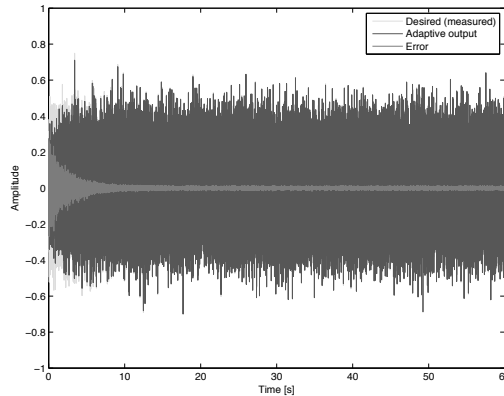


Figure 19: *Error of adaptive filter, linear circuit with pink noise as input.*

The error is clearly smaller, and therefore the nonlinear behaviour of the loudspeaker must be the reason for the remaining error in fig 18.

4.3.3 Impulse response processing

A filter length of 400 was chosen, as described in 4.3.1. This results in a filter that is approximately 180ms long, compared to the theoretical impulse response that is approximately 50ms long. Using white noise at a low level as input and looking at the impulse response after 30 seconds results in figure 20.

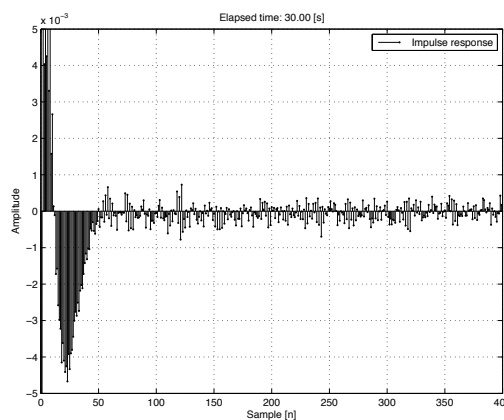


Figure 20: *Impulse response at $t=30s$, white noise at low level as input. Note the noisy signal at the end of the impulse. Zoomed y-axis.*

The signal is very noisy, and the impulse has not died out at the end. The solution should therefore be to use a longer filter, but this is not the case. The signal at the end should be considered to be noise. One argument for *not* considering it as noise is that a high input level still results in this type of ringing in the impulse response. The answer is therefore more likely that it is a result of the nonlinearities. Remember that the adaptive filter used is a linear filter and therefore cannot adapt to nonlinearities.

In order to get rid of the noise in the impulse response some processing is performed. First, the end of the impulse response is faded, to ensure that the impulse has died out. Secondly, a moving average is calculated, to smooth the response.

To fade the impulse response, a gain curve is calculated. The impulse is then multiplied with the gain curve to construct the faded impulse response. The gain curve is shown in figure 21. The first 250 samples have a gain of one. The last 150 samples are the last half of a Hann window.

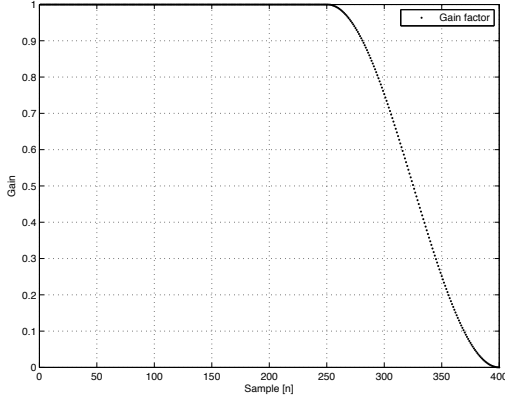


Figure 21: Gain curve for fading the impulse response. Fade is constructed with half of a Hann window and is 150 samples long.

A Hann window is calculated as

$$v(n) = 0.5 \left(1 - \cos \left(2\pi \frac{n}{N} \right) \right) \quad (27)$$

where $0 \leq n \leq N$ and the length of the window is $L = N + 1$. The last window coefficient $v(N)$ is always zero. In this way the impulse response is forced to stop ringing. Multiplying the noisy impulse response in figure 20 with the gaincurve in figure 21 results in a faded impulse response

shown in figure 22.

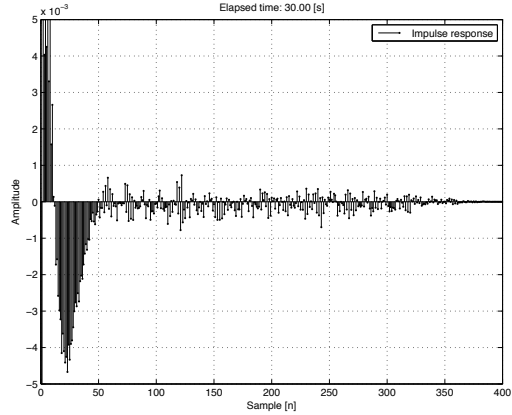


Figure 22: Faded impulse response, has magnitude 0 at last sample. Zoomed y-axis.

In order to further clean the impulse response a moving average using current and previous impulses is calculated. The number of impulses in the average is N and the current impulse-vector is $\hat{\mathbf{w}}[n]$. The average is calculated as

$$\hat{\mathbf{w}}_{avg}[n] = \frac{1}{N} \sum_{k=n-(N-1)}^n \hat{w}_i[k] \quad (28)$$

where i is the row index in the vector $\hat{\mathbf{w}}$. This results in a sliding window of length N and an averaged impulse response vector $\hat{\mathbf{w}}_{avg}$ for every block. An example is shown in figure 23 taken from an analysis where each block is one second long and $N = 5$. Compare figure 23 with figure 22 which is from the same set of data. The impulse response is more stable after the averaging.

Of course a smaller blocksize results in more impulse responses which then opens up for more averaging. A smoother impulse response is better, since the frequency response of the impulse response later will be used to calculate the impedance.

4.4 Curve fitting

The impulse response vector $\hat{\mathbf{w}}$ is the same as the filter coefficients. The complex frequency response is then calculated and this results in the admittance. An example of an adaptively estimated impedance is shown in figure 24. Music is used as input and the curve resembles the one

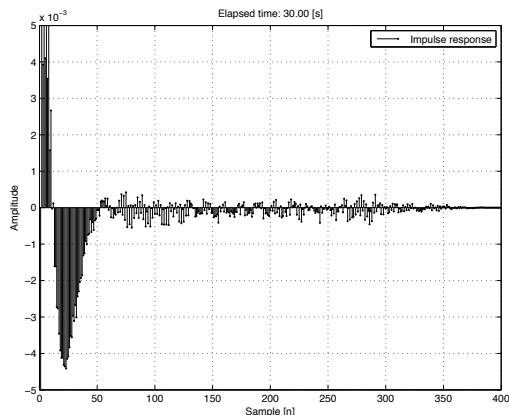


Figure 23: *Averaged impulse response, sliding window of current+4 previous impulses. Zoomed y-axis.*

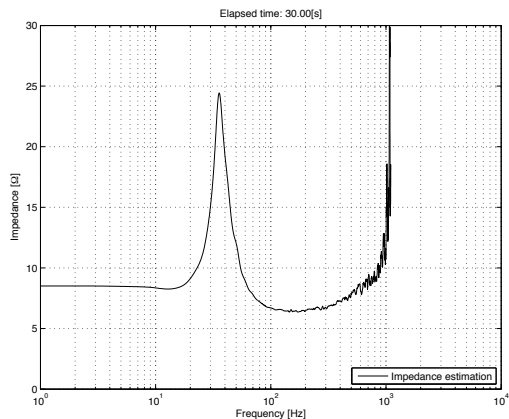


Figure 24: *Impedance derived from impulse response of adaptive filter. Note the rise in impedance at $f \approx 1\text{kHz}$. This is due to the anti-aliasing filter in the downsampling process.*

shown in figure 6. The rise to infinity at 1kHz is due to the anti-aliasing filter in the downsampling process. This also means that the inductance L_e is overestimated and therefore pushed higher than it actually is. Therefore the values close to $f_s/2$ must be considered not reliable. Here f_s means samplerate. Also most power amplifiers have a highpass filter at a frequency somewhere below 10Hz. The amplifier⁹ used in this thesis has a frequency range of 10Hz-20kHz +0/-0.3dB.

The valid frequency range is therefore set to be 15–600 Hz.

⁹Crest Audio Vs1500 <http://www.crestaudio.com>

A curve fitting algorithm is then applied to fit to the estimated impedance. The algorithm chosen is the Nelder–Mead simplex, described in appendix B. This is simply implemented in Matlab using `fminsearch` which uses the Nelder–Mead simplex to minimise a function. A function to be minimised is written, which is called the error function. The error is defined as

$$error = \sum_{i=1}^N (Z_i - \hat{Z}_i)^2 \quad (29)$$

where Z is the model impedance calculated with equation 9 and \hat{Z} is the adaptively estimated impedance and i is the frequency bin at which the impedances is compared. The five parameters in the model impedance Z are then modified (using `fminsearch`) until the error is small enough and then the model is fitted to the adaptive estimation. An example is shown in figure 25 which is the same adaptive estimation as in figure 24.

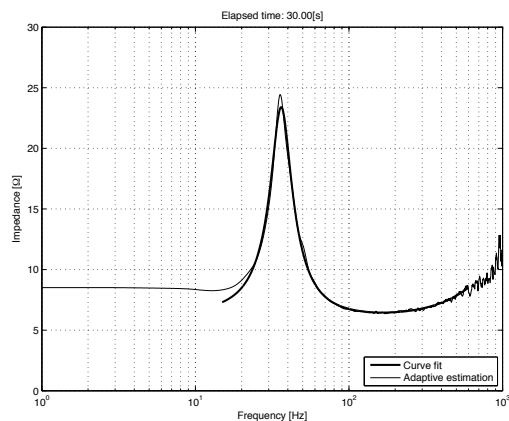


Figure 25: *Fitted model to adaptive estimation.*

In the block-based implementation described earlier a curve fit is performed at the end of each block and therefore results in an estimation of the impedance at each block. The five parameters are used as starting values for the curve fitting in the next block.

4.5 Temperature calculations

The only temperature-dependant parameter is R_e as described in 1.3.1. Each adaptive estimation of the impedance results in a curve fit which then results in the five linear loudspeaker parameters. Using equation 2 for each estimated

R_e results in figure 26. The actual temperature is also shown. The estimated temperature (based on the impulse responses from the adaptive filter) is lower than the actual temperature (measured with the thermocouple) and the error seems to be bigger at higher temperatures. This will be discussed in section 5.

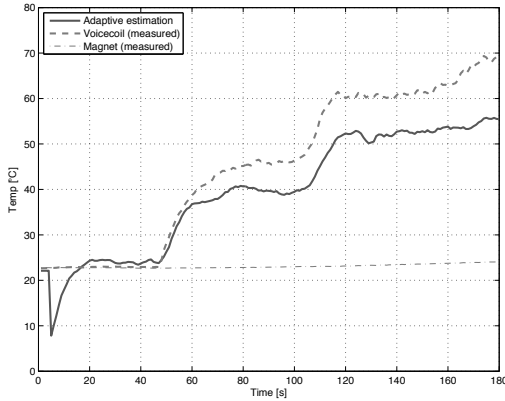


Figure 26: *Actual and estimated temperatures, music as source.*

Music is used as input and the estimated temperature tracks the big changes in temperature. The step-like behaviour in the temperature is simply an increase in volume into the power amplifier. A visual inspection on the error e from the adaptive filter yields that the error is too big during the first five seconds. The temperature is therefore set to the previous known value. At the beginning of an estimation that is set to room temperature. There is no point in doing any further analysis on the impulse response from the adaptive filter if the error e is too big.

After the first five seconds the filter is still trying to minimise the error e , but after 20 seconds the estimated temperature is correctly estimated as room temperature.

In order to investigate the temperature rise, a slowly increasing white noise signal was used to heat the voice-coil. The input signal can be seen in figure 27.

The temperature will slowly increase and the adaptive estimated temperature can be seen in figure 28. Even though the temperature is estimated correctly at room temperature, the error becomes bigger the higher the actual temperature in the voice-coil gets.

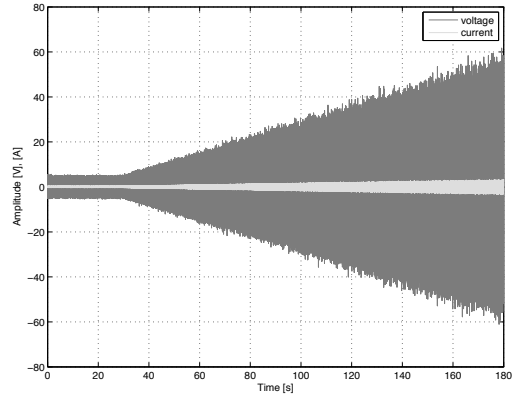


Figure 27: *White noise ramp input signal for slow heating of voice-coil.*

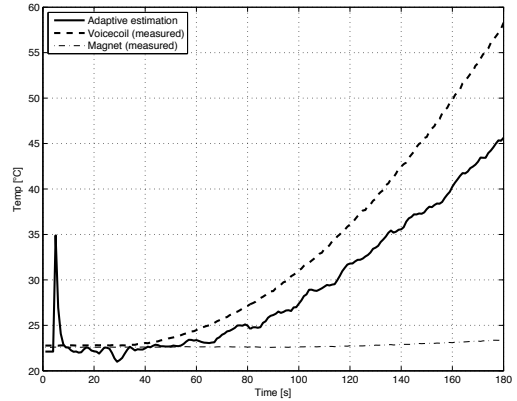


Figure 28: *Temperature estimation with white noise slowly increasing in amplitude.*

4.6 Resonance frequency shift

The change in resonance frequency was discussed in section 1.5. An example from a measurement with music is shown in figure 29. The figure shows two adaptive estimations with corresponding curve fit. The estimations are done at different times, the first when the input signal is at a low level and the second when the input signal is bigger.

The figure clearly shows the increase in R_e and also the shift in resonance frequency. The figure also shows that it is possible to track the changes in the impedance with music as an input.

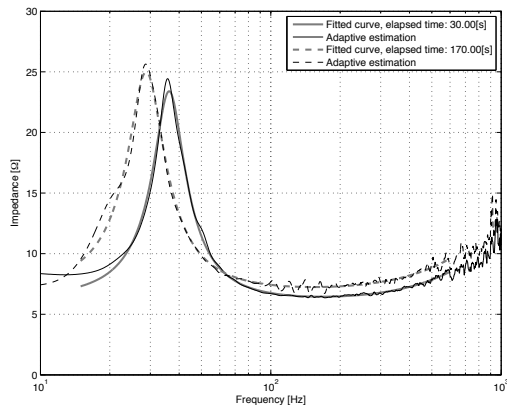


Figure 29: Impedance at low level input and a later high level input. Note the rise in DC-offset which is the change in R_e and also the shift downwards in resonance frequency.

5 Analysis and discussion

The figures shown in section 4 summarises the different measurements results. Different stimuli produces similar results. The temperature difference in figure 28 shows that at a known correct temperature of 58°C the estimated temperature is 45°C . A better accuracy must be achieved here in order for this method to be practically usable.

The inaccuracy is probably mostly due to the current measurement. In the calibration process described in section 3.2.3 some measurements were performed on a power-resistor array. After calibration, the correct values could be measured on the known power-resistor array. Changing the configuration on the power-resistor array to a higher (25%) value and then measuring again would result in a small error in the measured value. So the current and voltage measurement devices have an error that propagates through the rest of the system.

The temperature derived in section 4 is lower than the correct temperature. It starts somewhat at the correct temperature, but when the temperature rises the error gets bigger. The reason for this error can be many things, some will be discussed here. The biggest error is probably in the method of measuring the current. The voltage measurement is also a factor. The changes in R_e that is to be measured in this thesis is in the span of $0\text{-}1\Omega$. This is small changes in the resistance and even with a professional

multimeter these small changes can be difficult to measure accurately. A calibration error early in the process will propagate and be quite big at the end. The method of measuring the current with a shunt resistor can be tricky if it is badly designed. This is because the voltage changes measured over the shunt is small, since a small value on the shunt resistor must be used.

All parameters are calibrated at room temperature. When the temperature rises it cannot be guaranteed that it is only R_e that changes. An increasing current will also heat the shunt resistor R_7 and therefore its resistance will change according to equation 2. The relationship between R_e and temperature has been widely used and has been verified by others.

The adaptive filter used is a linear filter, whereas the loudspeaker behaves nonlinear even at a small displacement. So the error from the adaptive filter will always be relatively big. It does not matter if a different linear adaptive filter is used, because it will always be a *linear* filter. Using averaging somewhat minimises the error caused by nonlinearities, but it will not completely remove it. The resulting impedance estimation is quite stable over time, even with music as an input.

Using thermal modelling results in a very good accuracy, Chapman [13] states an error less than 2°C for his thermal model. This type of accuracy has not been seen in the adaptive parameter estimation method.

The adaptive filter used here is ideally driven by a random signal like white noise. Music is not random and a signal with narrow frequency spectrum will result in an erroneously impulse response estimation of the loudspeaker.

In the process of finding the value of R_e for calculating the temperature increase, all linear loudspeaker parameters are estimated. This is a bonus as the parameters describe the impedance of the loudspeaker when music is used as an input. The benefit of knowing the impedance is for example that compensation for thermal compression can be performed.

5.1 Verification of results

The linear parameters was measured with a Klippel Distortion Analyzer¹⁰ and this system delivers a set of both linear and nonlinear parameters. The linear parameters are presented after a multi-tone measurement. Since there is a measurement error in the adaptive estimation procedure, there is no point in strictly comparing values between the two methods. Still the adaptive parameters estimated in this thesis are close to the parameters estimated with the Klippel system. The estimated set of parameters are also verified in the sense that the resulting impedance looks normal. A system for estimating the linear loudspeaker parameters in real-time does not exist today, and therefore a verification is difficult to do.

The temperature estimation is verified by the measurement done with the thermocouple in the voice-coil. The correctness of this measurement system has been discussed in section 3.3.2.

6 Future work

For future work, some items are suggested. In summary, the current and voltage must be measured correctly and the use of more complex adaptive filters needs to be investigated.

- The most important factor for future work would be a correct measurement system for accurate measurements of the current and the voltage.
- Using the simple NLMS adaptive filter has its advantages, but investigating a more complex adaptive filter, like the Kalman filter, would result in the estimation of the parameters already in the adaptive filter. This means that the time-consuming curve fit does not have to be performed.
- The Nelder–Mead simplex method for finding the minimum of a function is known for its inefficiency. If a curve fit still has to be performed there exist more efficient methods.
- Expanding the model to include some nonlinear parameters. Those parameters could

be modelled relative to displacement x of the diaphragm and taken from a look-up table.

- A nonlinear adaptive filter could be used. The extended Kalman filter is also an option.
- An implementation in a DSP for realtime estimation. The above described methods are all performed off-line and are somewhat time-consuming.

7 Acknowledgements

This work has been performed at Bang & Olufsen in Struer, Denmark and at Luleå University of Technology in Luleå, Sweden. Thanks to Gert Munch, Peter Chapman and John Madsen, all of B&O, for help during the project.

Especially thanks to Sylvain Choisel and Jakob Dyreby at B&O for ideas and endless discussions, usually started by the author with the words "do you have a minute?".

¹⁰<http://www.klippel.de>

References

- [1] John King. Loudspeaker voice coils. *J. Audio Eng. Soc.*, 18(1):34–43, February 1970.
- [2] A. Neville Thiele. Loudspeakers in vented boxes: Part 1. *J. Audio Eng. Soc.*, 19(5):382–392, May 1971.
- [3] A. Neville Thiele. Loudspeakers in vented boxes: Part 2. *J. Audio Eng. Soc.*, 19(6):471–483, June 1971.
- [4] Richard H. Small. Direct-radiator loudspeaker system analysis. *J. Audio Eng. Soc.*, 20(5):383–395, June 1972.
- [5] Richard H. Small. Closed-box loudspeaker systems part 1: Analysis. *J. Audio Eng. Soc.*, 20(10):798–808, December 1972.
- [6] Richard H. Small. Closed-box loudspeaker systems part 2: Synthesis. *J. Audio Eng. Soc.*, 21(1):11–18, January/February 1973.
- [7] Gottfried Behler. Measuring the loudspeaker’s impedance during operation for the derivation of the voice coil temperature. In *Audio Eng. Soc. preprint*, number 4001 in 98th AES Convention, Paris, France, February 1995.
- [8] John Vanderkooy. A model of loudspeaker driver impedance incorporating eddy currents in the pole structure. *J. Audio Eng. Soc.*, 37(3):119–128, March 1989.
- [9] Julian R. Wright. An empirical model for loudspeaker motor impedance. *J. Audio Eng. Soc.*, 38(10):749–754, October 1990.
- [10] W. Marshall Leach Jr. Loudspeaker voice-coil inductance losses: Circuit models, parameter estimation, and effect on frequency response. *J. Audio Eng. Soc.*, 50(6):442–450, June 2002.
- [11] Ning Wu, Yong Shen, and Xiaobing Xu. A study on lumped elements model and thermal effects of eddy currents in loudspeakers. In *Audio Eng. Soc. preprint*, number 6575 in 119th AES Convention, New York, USA, October 2005.
- [12] Clifford A. Henricksen. Heat-transfer mechanisms in loudspeakers: Analysis, measurement, and design. *J. Audio Eng. Soc.*, 35(10):778–791, October 1987.
- [13] Peter Chapman. Thermal simulation of loudspeakers. In *Audio Eng. Soc. preprint*, number 4667 in 104th AES Convention, Amsterdam, May 1998.
- [14] Peter Chapman. Complete thermal protection of an active loudspeaker. In *Audio Eng. Soc. preprint*, number 5112 in 108th AES Convention, Paris, France, February 2000.
- [15] Fabio Blasizzo. A new thermal model for loudspeakers. *J. Audio Eng. Soc.*, 52(1/2):43–55, January/February 2004.
- [16] Wolfgang Klippel. Nonlinear modeling of the heat transfer in loudspeakers. *J. Audio Eng. Soc.*, 52(1/2):3–25, January/February 2004.
- [17] Douglas J. Button. Heat dissipation and power compression in loudspeaker. *J. Audio Eng. Soc.*, 40(1/2):32–41, January/February 1992.
- [18] Bo Rohde Pedersen and Per Rubak. Musical transducer-less identification of linear loudspeaker parameters. In *Audio Eng. Soc. preprint*, 32nd International AES Conference, 2007.
- [19] John P. Bentley. *Principles of Measurement Systems*. Pearson Education Limited, 2005.
- [20] Simon Haykin. *Adaptive Filter Theory*. Pearson Education Limited, 2002.

A Adaptive filter theory

The theory behind adaptive filters is described in details by Haykin[20] and a brief description will be given here. An adaptive filter can be successfully used to track changes in an unknown system.

The theory presented here is applicable on discrete-time systems, but in general adaptive filters can be applied on continuous-time systems as well.

The unknown system is usually called *plant* in the context of adaptive filters. There is four basic classes of adaptive filters and the one used in this thesis is the one called *Identification*. The adaptive filter is used to estimate a linear model that in some sense provides the best fit to the unknown plant. The plant is assumed to be a linear system. Both plant and adaptive filter is fed with the same input u and the output from the plant is called the *desired* response d . The output y from the adaptive filter is used to calculate the estimation error $e = d - y$. Summary of notation used:

- u = input applied to the adaptive filter
- y = output from the adaptive filter
- d = desired response
- e = estimation error $e = d - y$

The setup for *Identification* is shown in figure 30. The adaptive filter will try to minimise the error e by matching the impulse response of the plant. The method of minimising the error is a design choice. Two popular methods is described in the next section.

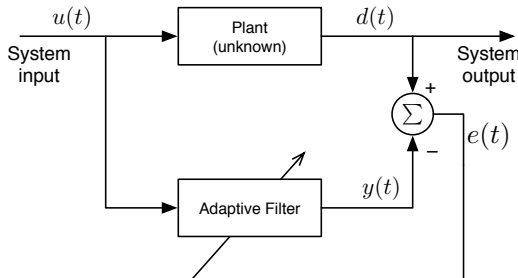


Figure 30: Adaptive filter for identifying a linear unknown system.

If the plant is slowly changing its parameters

over time then the adaptive filter will track that change.

A.1 Least Mean Square

The LMS, Least Mean Square, algorithm is a popular method for implementing an adaptive filter. Its popularity is mostly due to its simplicity.

The input vector

$$\mathbf{u}[n] = \begin{bmatrix} u[n] \\ u[n-1] \\ \vdots \\ u[n-(M-1)] \end{bmatrix} \quad (30)$$

is the current input and $M-1$ previous samples, where M is the length of the filter. The tap-weight (coefficients) vector $\hat{\mathbf{w}}[n]$ is of length M and contains the estimated coefficients at time n . Since the filter is an FIR (Finite Impulse Response) filter, the coefficients is the same as the impulse response. If there exists no previous knowledge about the tap-weights, then

$$\hat{\mathbf{w}}[0] = \mathbf{0} \quad (31)$$

is used.

The output from the filter is

$$y[n] = \hat{\mathbf{w}}^H[n] \mathbf{u}[n] \quad (32)$$

where the superscript H denotes Hermitian transposition. A Hermitian transposition consists of transposition and complex conjugation. If the input and the tap-weights are real, a simple transposition is enough. Then equation 32 becomes

$$y[n] = \hat{\mathbf{w}}^T[n] \mathbf{u}[n]. \quad (33)$$

The error is defined as the difference between the desired signal and the output from the filter,

$$e[n] = d[n] - y[n]. \quad (34)$$

The next estimation of the tap-weights is then

$$\hat{\mathbf{w}}[n+1] = \hat{\mathbf{w}}[n] + \mu \mathbf{u}[n] e^*[n] \quad (35)$$

where μ is the *step-size* and the asterisk $*$ denotes complex conjugation. The error e will be real if the desired and the filter output is real.

The step-size μ determines the rate of convergence for the filter. A small step-size means that the filter will converge slowly and a large step-size will cause the filter to become unstable. In order to be stable, the step-size is bound to be within

$$0 < \mu < \frac{2}{MS_{max}} \quad (36)$$

where S_{max} is the maximum value of the power spectral density of the tap inputs $u[n]$ and the filter length M is moderate to large.

A.2 Normalised Least Mean Square

When calculating the adjustment for the tap-weights $\hat{\mathbf{w}}[n]$ in the LMS filter, the adjustment is directly proportional to the input $\mathbf{u}[n]$. Therefore, when $\mathbf{u}[n]$ contains large values the LMS filter suffers from a gradient noise amplification problem. The Normalised LMS filter overcomes that problem by using a *time-varying step-size parameter*. The structure of a NLMS filter is exactly the same as for the LMS filter.

The time-varying step-size calculated as

$$\mu = \frac{\tilde{\mu}}{\|\mathbf{u}[n]\|^2} \quad (37)$$

where $\tilde{\mu}$ is the adaptation constant and the step-size is normalised with respect to the squared Euclidian norm of the input $\mathbf{u}[n]$, hence the term *normalised*.

The tap weight vector $\hat{\mathbf{w}}[n+1]$ is therefore calculated as

$$\hat{\mathbf{w}}[n+1] = \hat{\mathbf{w}}[n] + \frac{\tilde{\mu}}{\|\mathbf{u}[n]\|^2} \mathbf{u}[n]e^*[n] \quad (38)$$

in which the similarities with equation 35 is obvious, the difference is the normalised step-size.

The gradient noise amplification problem is solved in the NLMS, but the normalisation introduces a new problem. When the input $\mathbf{u}[n]$ is small, the division by the squared norm $\|\mathbf{u}[n]\|^2$ becomes small and therefore numerical problems may arise. By introducing a constant $\delta > 0$ in equation 38 this can be solved;

$$\hat{\mathbf{w}}[n+1] = \hat{\mathbf{w}}[n] + \frac{\tilde{\mu}}{\delta + \|\mathbf{u}[n]\|^2} \mathbf{u}[n]e^*[n]. \quad (39)$$

The adaptation constant $\tilde{\mu}$ is bound to be within

$$0 < \tilde{\mu} < 2 \frac{E[|u(n)|^2]\mathcal{D}(n)}{E[|e(n)|^2]} \quad (40)$$

where $E[|u(n)|^2]$ is the input signal power, $E[|e(n)|^2]$ is the error signal power and $\mathcal{D}(n)$ is the mean square deviation.

A great benefit from using the NLMS over the LMS is that the rate of convergence is potentially faster for both uncorrelated and correlated input data.

B Function minimisation

There exist several methods to find the global minimum of a function. It can be done both analytically and numerically by the use of gradients. It can also be done without the use of gradients and is then usually called *direct search* methods.

B.1 Nelder–Mead algorithm

If only the function values are present then the simplex method described by the Nelder–Mead algorithm can be used. This is a direct search method that does not rely on gradients.

A *simplex* is a polytope of $N + 1$ vertices in N -space. In two dimensional space it is a triangle and in three dimensional space it is a tetrahedron (pyramid). The number of parameters determines N . At each step of the search the function value at a new point in the vicinity of the simplex is calculated. The new point is compared to the function values at the vertices of the simplex. If the new point has a smaller value then it is used to replace one of the vertices to form a new simplex. If not, a new point is tested. If the difference between the values at the vertices is small then the simplex is shrunken. The search continues until the size of the simplex is smaller than the tolerance specified.

As for all general purpose methods the simplex can get stuck in a local minimum. To handle this problem the simplex can be restarted at the current best value.